POTSDAM-INSTITUT FÜR KLIMAFOLGENFORSCHUNG

Originally published as:

Franke, J. A., Müller, C., Minoli, S., Elliott, J., Folberth, C., Gardner, C., Hank, T., Izaurralde, R. C., Jägermeyr, J., Jones, C. D., Liu, W., Olin, S., Pugh, T. A., Ruane, A. C., Stephens, H., Zabel, F., Moyer, E. J. (2022): Agricultural breadbaskets shift poleward given adaptive farmer behavior under climate change. - Global Change Biology, 28, 1, 167-181.

DOI: https://doi.org/10.1111/gcb.15868

PRIMARY RESEARCH ARTICLE

Agricultural breadbaskets shift poleward given adaptive farmer behavior under climate change

James A. Franke[1,2] | Christoph Müller[3] | Sara Minoli[3] | Joshua Elliott[2] | Christian Folberth[4] | Charles Gardner[5] | Tobias Hank[6] | R. Cesar Izaurralde[7] | Jonas Jägermeyr[8,3,9] | Curtis D. Jones[7] | Wenfeng Liu[10] | Stefan Olin[11] | Thomas A.M. Pugh[11,12,13] | Alex C. Ruane[8] | Haynes Stephens[1,2] | Florian Zabel[6] | Elisabeth J. Moyer[1,2,*]

[1]Department of the Geophysical Sciences, University of Chicago, Chicago, USA

[2]Center for Robust Decision-making on Climate and Energy Policy (RDCEP), University of Chicago, Chicago, USA

[3]Potsdam Institute for Climate Impact Research (PIK), Member of the Leibniz Association, Potsdam, Germany

Correspondence
Elisabeth J. Moyer, Department of the Geophysical Sciences, University of Chicago, Chicago, USA
Email: moyer@uchicago.edu

Funding information
NSF grant SES-1463644, NSF NRT program (grant no. DGE-1735359), NSF Graduate Research Fellowship Program (grant no. DGE-1746045). NASA NNX16AK38G (INCA). European Research Council Synergy (grant no. ERC-530 2013-SynG-610028 Imbalance-P).

Modern food production is spatially concentrated in global "breadbaskets". A major unresolved question is whether these peak production regions will shift poleward as the climate warms, allowing some recovery of potential climate-related losses. While agricultural impacts studies to date have focused on currently cultivated land, the Global Gridded Crop Model Intercomparison Project (GGCMI) Phase 2 experiment allows us to assess changes in both yields and the location of peak productivity regions under warming. We examine crop responses under projected end-of-century warming using 7 process-based models simulating 5 major crops (maize, rice, soybeans, and spring and winter wheat) with a variety of adaptation strategies. We find that in no-adaptation cases, when planting date and cultivar choices are held fixed, regions of peak production remain stationary and yield losses can be severe, since growing seasons contract strongly with warming. When adaptations

in management practices are allowed (cultivars that retain growing season length under warming and modified planting dates), peak productivity zones shift poleward and yield losses are largely recovered. While most growing-zone shifts are ultimately limited by geography, breadbaskets studied here move poleward over 600 km on average by end of the century under RCP8.5. These results suggest that agricultural impacts assessments can be strongly biased if restricted in spatial area or in the scope of adaptive behavior considered. Accurate evaluation of food security under climate change requires global modeling and careful treatment of adaptation strategies.

KEYWORDS
crop modeling, climate change, adaptation, AgMIP, GGCMI

[4]Ecosystem Services and Management Program, International Institute for Applied Systems Analysis, Laxenburg, Austria [5]Program on Global Environment, University of Chicago, Chicago, USA [6]Ludwig-Maximilians-Universität München (LMU), Munich, Germany [7]Department of Geographical Sciences, University of Maryland, College Park, MD, USA [8]NASA Goddard Institute for Space Studies, New York, USA [9]Columbia University Center for Climate Systems Research, New York, USA [10]]College of Water Resources and Civil Engineering, China Agricultural University, Beijing 100083, China [11]Department of Physical Geography and Ecosystem Science, Lund University, Lund, Sweden [12]School of Geography, Earth and Environmental Sciences, University of Birmingham, Birmingham, UK [13]Birmingham Institute of Forest Research, University of Birmingham, Birmingham, UK

1 | INTRODUCTION

While agriculture is widespread on the Earth's surface, food production is spatially concentrated: 80% of global cereals (and soybeans) and nearly half of total global calories are produced from just ~3% of ice-free land surface area (SPAM, International Food Policy Research Institute, 2019), largely concentrated in temperate "breadbaskets" or "rice bowls". From the beginnings of modern climate science, there has been concerns that climate change would drive these regions of optimal cultivation poleward, causing significant economic disruptions. Newman (1980) estimated that a 1°C increase in daily temperature could shift the North American maize belt poleward by 175 km, and other studies in the 1980s found similar effects (e.g. Blasing and Solomon, 1983; Rosenzweig, 1985; Warrick, 1988). A large body of work since then has continued this approach of evaluating potential changes in agricultural suitability (e.g. Akpoti et al., 2019, and references therein). While many studies use suitability rules based only on mean temperature and precipitation (e.g. Caviezel et al., 2017; King et al., 2018; Hannah et al., 2020), others incorporate soil characteristics (e.g. Zabel et al., 2014) or employ more complex climate suitability approaches (e.g. He and Zhou, 2012; Zhang et al., 2017; Ramirez-Cabral et al., 2017; Kogo et al., 2019; Hoffman et al., 2020). In economics, rule-based suitability maps have been used to investigate how future climate-driven changes in production across countries may impact the global food trade (e.g. Costinot et al., 2016; Hertel, 2018). However, while climate change is already modifying the

spatial distributions of many species of plants and animals (e.g. Parmesan, 2006, and references therein), evidence for real-world shifts in agricultural growing zones is more limited (Sloat et al., 2020).

Despite the concern about shifting "breadbaskets", nearly all modeling assessments of the impacts of climate change on crop yields consider production only on currently cultivated land (e.g. Müller and Robertson, 2014). Many studies of future yields use statistical models trained on historical records of crop yields and weather, an approach that can only produce predictions over regions where those records exist (e.g. Schlenker and Roberts, 2009; Moore et al., 2017b; Anderson et al., 2019; Gaupp et al., 2020; Kornhuber et al., 2020; Qin et al., 2020). These empirical approaches cannot test whether optimal production zones may shift into regions where crops are not currently grown. By contrast, process-based simulation models often produce global output, but in reporting production changes, typically focus on current cultivation where models are more skillful (e.g. Rosenzweig et al., 2014; Asseng et al., 2015, 2019; Jägermeyr et al., 2021; Müller et al., 2021). Both "static" approaches – empirically-based statistical models and process-based models run over currently cultivated land – tend to project significant yield losses under expected climate change when effects of [CO_2] fertilization are neglected (e.g. Zhao et al., 2017). In the more realistic case of including [CO_2] (Toreti et al., 2020), yield responses are mixed, often with different directions of change for specific regions and crops (Rosenzweig et al., 2014; Jägermeyr et al., 2021).

In reality, the climate-induced shift in optimal production zones will likely fall between the "perfect" shift implied by the suitability approach and the stasis assumed in most impact assessments. Climate-suitability approaches still have difficulty including limiting factors such as various soil characteristics, precipitation variability, and total radiation. Global process-based models incorporate all of these physical factors, and in theory could accurately map evolving spatial patterns of crop yields, but in practice are limited by difficulties in accounting for human factors instead. Management choices such as planting dates and cultivar characteristics (which determine harvest dates) are typically specified for each geographic region based on current data and hard-wired into the model parameters. (Some previous studies have partially implemented a dynamic planting date within a fixed historical window (Rosenzweig et al., 2014).) The models therefore preclude the dynamic behavioral responses needed to capitalize on changing suitability. Typically, growing seasons are shorter and start later in the year in higher latitude production zones, reflecting the seasonal cycle. For example, maize planting starts in May in North Dakota, 1 month later than in Missouri (USDA National Agricultural Statistics Service, 2020), to avoid late frosts. Crop models cannot realistically capture changes in future spatial patterns of yields as the climate warms without relaxing that constraint on growing season start and length. For this reason, it is unsurprising that several recent studies using yield projections from process-based models without adaptations find little geographic shift of production under warming (Stevanović et al., 2016). Even when a crop models with dynamical planting date in a fixed window is employed within an economic model (e.g Janssens et al., 2020), little production shift was found under warming.

Recent experiments with global crop model ensembles that explicitly consider growing season adaptations now allow evaluating the factors that control poleward agricultural shifts. In this study we utilize seven process-based crop models that participated in the Global Gridded Crop Model Intercomparison Project (GGCMI) Phase 2 (Elliott et al., 2015; Müller et al., 2017; Franke et al., 2020a) to test how the shift of peak agricultural productivity regions depends on treatment of farmer adaptation.

2 | MATERIALS AND METHODS

2.1 | Crop model simulations

This analysis utilizes simulations compiled as part of GGCMI Phase 2 (Franke et al., 2020a,b), an exercise involving widely-used mechanistic process-based crop models conducted within the Agricultural Model Intercomparison and Improvement Project (AgMIP) (Rosenzweig et al., 2013; Ruane et al., 2017). Of the 12 models participating in GGCMI Phase 2, we use 7 here (Table 1), excluding 3 that provided insufficient simulations and 2 that used non-harmonized treatment of growing season length (see below). We also analyze an additional set of simulations by one of the GGCMI models, LPJmL (the Lund-Potsdam-Jena managed Land model), that includes more detailed growing period adaptation representation (Table 2). All models represent a suite of biophysical processes including photosynthetic light utilization, soil water and nutrient dynamics, phenological development, heat and water stress, evapotranspiration, and CO_2 effects. All models simulated maize, rice, soybean, and spring and winter wheat other than LPJ-GUESS, which omitted rice and soybean. Simulations were run at 0.5 degree spatial resolution and cover over 80% of the Earth's land surface, including all cultivated land, 58% of land surface area, and much uncultivated land, excluding areas judged unsuitable for cultivation under any climate scenario. See Franke et al. (2020a) for details.

TABLE 1 The 7 process-based globally gridded crop models used in the study, which fall into two categories. *Site-based* models were originally developed for field-level simulations and typically involve more detail on cropping systems. *Ecosystem* or land surface models were originally developed to represent the natural terrestrial biomes and typically involve a more detailed representation of the water cycle. PROMET was originally developed from an hydrological model but is now an intermediate case.

Model	Key citations	Model type
pDSSAT	Elliott et al. (2014); Jones et al. (2003)	Site-based
EPIC-TAMU	Izaurralde et al. (2006)	Site-based
GEPIC	Liu et al. (2007); Folberth et al. (2012)	Site-based
PEPIC	Liu et al. (2016a,b)	Site-based
LPJmL	von Bloh et al. (2018)	Ecosystem
LPJ-GUESS	Lindeskog et al. (2013); Olin et al. (2015)	Ecosystem
PROMET	Hank et al. (2015); Mauser et al. (2015); Zabel et al. (2019)	Site-based/Ecosystem

In GGCMI Phase 2, runs were conducted with uniform perturbations applied to a 30-year timeseries of historical climate inputs. Most models use daily data from the NASA AgMERRA 0.5 degree gridded reanalysis product (Ruane et al., 2015), but PROMET uses sub-daily data from the WFDEI climate dataset Weedon et al. (2014). The experimental protocol involved 9 levels for precipitation, 7 for temperature, 4 for [CO_2] and 3 for applied nitrogen, for a total of 672 simulations for rain-fed agriculture and an additional 84 for irrigated crops. Perturbations are uniform in space and therefor represents a possible climate future that could occur in each individual gridcell, but not one which would occur simultaneously across all gridcells. (See Franke et al. (2020b) for more details.) All simulations are run twice, first with present-day cultivar genetics and then with assumed cultivar adaptations. The additional LPJmL simulations involve more extensive treatment of growing period adaptation. These simulations are driven by climate projections from 4 CMIP5 models under the RCP8.5 scenario. Representation of growing season adaptation in both datasets is described in more detail below and in supplementary material section 1.

TABLE 2 The process-based crop model scenarios presented in this analysis.

Scenario	Climate input	Model configuration	Models included
GGCMI Phase 2 baseline **(A0)**	Uniform perturbations in temperature applied to historical reanalysis.	Phenology parameters held fixed. No adaptation measures.	pDSSAT, EPIC-TAMU, GEPIC, PEPIC, LPJmL, LPJ-GUESS, PROMET
GGCMI Phase 2 adaptation **(A1)**	Uniform perturbations in temperature applied to historical reanalysis.	Phenology parameters adjusted to maintain historical growing season length under warming.	pDSSAT, EPIC-TAMU, GEPIC, PEPIC, LPJmL, LPJ-GUESS, PROMET
No adapation	CMIP5, 4 climate models under RCP8.5.	Phenology parameters held fixed. No adapation measures.	LPJmL only
Planting advance	—"—	Planting day dynamically advanced under warming.	—"—
Harvest delay	—"—	Phenology parameters adjusted to maintain historical growing season length.	—"—
Full adaptation	—"—	Planting day dynamically advanced under warming and phenology parameters adjusted to maintain historical growing season length.	—"—
Full adaptation + uniform soils and radiation	—"—	—"— + Central Iowa soils and radiation are applied everywhere.	—"—

In the GGCMI Phase 2 historical base case, models are harmonized to match the same region- and crop-specific planting and harvest dates (Elliott et al., 2015). For all models, crop phenology parameters (e.g. phenological heat unit requirements) were calibrated to match harmonized calendars, largely adapted from the SAGE (Center for Sustainability and the Global Environment, University of Wisconsin) crop calendar (Sacks et al., 2010). See Franke et al. (2020a) for crop calendar details and its Supplementary Section S3 and Table S1 for crop-specific parameters and details on the process for tuning each model. In the no-adaptation GGCMI Phase 2 simulations (termed "A0"), with phenological parameters left unchanged from the historical case, growing periods shrink under warming because crop development accelerates. In the adaptive cultivar choice simulations (termed "A1"), models are re-parameterized for each temperature level to delay crop maturity and maintain the original growing period length (averaged across each 30 year simulation). Note that the A1 runs capture only partial adaptation, since the planting date is left fixed at its historical values regardless of warming. Even so, adaptation substantially reduces warming-related yield reductions on currently cultivated land (Minoli et al., 2019b; Zabel et al., 2021, this issue).

Additional LPJmL simulations involve more extensive treatment of cultivar adaptation beyond delaying maturity. The LPJmL model uses a rule-based parameter adjustment (Waha et al., 2012; Minoli et al., 2019a) that can dynamically adjust both crop phenological parameters and planting and harvest dates as climate changes. Simulations shown here are run over two 20-year periods, 1985–2005 ("present") and 2080–2099 ("future"), with parameters set according to the 20-year mean climate. We explore 5 cases with the LPJmL model: 1) a *no-adaptation* case that utilizes the same historical growing seasons as the GGCMI Phase 2 protocol and keeps phenological parameters fixed, as in A0, so that

growing seasons shorten under warming; 2) a *maturity delay* case in which the required accumulated phenological heat units (PHU) at maturity are adjusted to maintain growing season length, as in A1; 3) a *planting advance* case in which phenological parameters are fixed but planting date is adjusted (typically advanced) under warming according to rules based on mean temperature and precipitation (Waha et al., 2012); 4) a *plant & maturity* case that combines the planting date change of 3) and cultivar modification of 2) Minoli et al. (2019a); and finally, for exploring the factors controlling breadbasket locations, 5) a *soils & radiation* case that combines the full *plant & maturity* adaptations of 4) with global soils and radiation set to the values in central Iowa, the heart of the North American maize breadbasket. (Soil input data are sourced from the Harmonized World Soil Database (HWSD Fischer et al., 2008), from the ISRIC-WISE database (Batjes, 2016), or from Shangguan et al. (2014) depending on individual crop model requirements, see Franke et al. (2020a) for details.) LPJmL planting date rules are location-specific and consider both temperature and precipitation. In the extra-tropics, where the dominant seasonal change is in temperature, crops are sown when the 30-year average of daily mean temperatures cross a crop-specific threshold, for example 14°C for maize and 18°C for rice. for rice (see Waha et al. (2012) for details). In the tropics, where precipitation cycles play a larger role, crops are sown at the onset of the rainy season. See Waha et al. (2012) for details on planting dates and Minoli et al. (2019a) for details on maturity dates, though note that LPJmL was run with slightly modified rules on maturity dates since this description. These adaptation cases are more extensive than most prior studies, but are still necessarily simplistic (e.g Challinor et al., 2018).

All LPJmL simulations are run under both dynamic [CO_2], matching that in climate projections, and fixed [CO_2]. This choice does not affect growing season timing, since the LPJmL growing-season rules are functions only of temperature and precipitation. Similarly, the GGCMI phase 2 protocol varies temperature and [CO_2] independently, and so provides simulations at a given degree of warming at a variety of [CO_2] levels from low (360 ppm) to high (810 ppm). While elevated [CO_2] can strongly affect yields, its effects are largely uniform in space, and therefore produce little change in the *relative* latitudinal distribution of potential yields. Models also disagree considerably in the impacts of [CO_2], so that varying [CO_2] in the analysis complicates the model comparison. For these reasons we predominantly show here results using fixed [CO_2], but show in Supplemental Material figures analogous figures using dynamic or elevated [CO_2]. The LPJmL fixed-[CO_2] simulations use the 2005 value of 380 ppm; in the GGCMI Phase 2 simulations, the "low" case uses the mean over the 1980–2010 period, 360 ppm. In Supplemental Material we show LPJmL simulations under the RCP8.5 scenario, where [CO_2] in the 2080-2099 "future" period ranges from 760 to 935 ppm, with a mean of 845 ppm, and the GGCMI Phase 2 case where warming of T+6°C is paired with 810 ppm [CO_2]. For comparison, we also show lower levels of warming (+2°C) at fixed [CO_2] (360 ppm) in order to discuss the robustness of our findings on the shift of peak productivity regions against these choices.

In this analysis, we use only crop model projections for the case of high nitrogen input, at 200 kgN ha^{-1}, so that current spatial patterns in fertilizer inputs do not confound our analysis. This choice implicitly assumes that farmers will be able to provide all necessary inputs to exploit the climatic potentials at any point in time.

2.2 | Breadbasket analysis

Breadbaskets have been defined in many ways in previous studies (e.g Bagley et al., 2012; Gaupp et al., 2020). Broadly, a breadbasket is defined as a localized area with especially high production of an individual crop within a region. However, the scale of analysis is a subjective choice, and while some methodologies result in six global "breadbaskets" for maize – North America, North China Plain, Western Europe, Northern India, Brazil, and Argentina (Gaupp et al., 2020) – many smaller regional areas of concentrated production are also often characterized as breadbaskets (e.g. the San Joaquin valley in California). In this analysis, we define a breadbasket as those gridcells in the top 10% of simulated

yields for a given crop in a continent-scale region. This definition is in line with the scale of analysis in previous studies of North America and Western Europe (e.g. Kornhuber et al., 2020) though slightly larger than that in studies of South America and East Asia (e.g. Gaupp et al., 2020). The breadbasket center is taken as the mean latitude and longitude of those gridcells in the top yield decile. Analysis here focuses on a few areas of strong importance to global food supply: primarily the North American maize belt, but with comparisons to wheat in Europe, soybeans in South America, and rice in East Asia. When comparing model output to maps of real-world data, we define the real-world breadbasket as the most intensely cultivated regions equivalent to a similar total area: for the N. American maize belt, ~165 Mha (million hectares) total area, of which 30 Mha is cultivated in maize.

For consistency, when evaluating changes in breadbasket locations under warming scenarios, we compare model-specific results with "future" and "present" simulations for each model, so that any model errors in spatial locations do not overly distort the analysis. Global gridded crop models do differ in their patterns of potential yields under present-day conditions, and in some cases appear to deviate from observed real-world cultivation patterns. For North American maize, for example, all models except pDSSAT place many of the best-yielding gridcells further south than the real-world maize belt. This mis-location of optimal growing locations appears amplified in ecosystem-type models (Supplemental Figure S3). Model skill at simulating present-day spatial yield patterns has been less well-tested than their skill at capturing year-to-year variation in country-level production, but differences are expected due to lack of detailed input data on management practices and cultivars (e.g. Elliott et al., 2015; Müller et al., 2017; Iizumi et al., 2018; Folberth et al., 2019). However, all models do reproduce strong spatial differences in yield and concentrated areas of optimal production.

Breadbasket temperature is reported as the mean growing period temperature in those gridcells in the top yield decile. When showing climatological future breadbasket temperature increases, we use the location of the future breadbasket, but compute temperatures over fixed historical growing seasons for consistency. Dynamic growing seasons and adaptive changes in planting date would make realized temperature increases smaller; see Supplemental Figure S25. We do not show temperature increases for wheat, because adaptations in wheat production may also involve changes from winter to spring wheat and vice versa.

3 | RESULTS

3.1 | Expected future growing-season climate changes

In a simple climate suitability framework, expected end-of-century climate change would imply substantial geographic shift of breadbaskets. To illustrate this, we show the case for maize in North America in Figure 1. While maize is the second-most widely grown crop globally, with almost 200 Mha (Food and Agriculture Organization of the United Nations (FAO), 2020) under cultivation, its production is highly concentrated, and the relatively small U.S. corn belt accounts for a full third of global production (Wang et al., 2020). The center of the U.S. corn belt is the state of Iowa, which produces 2.5 $\times$ as much corn as all of Mexico (Food and Agriculture Organization of the United Nations (FAO), 2020; USDA National Agricultural Statistics Service, 2020)). The compact size of the corn belt means that the vast majority of U.S. maize is grown at temperatures similar to those in Iowa: the standard deviation of corn belt mean growing season temperatures is only 2.3°C around the Iowa mean of ~21°C (AgMERRA, Ruane et al., 2015) (Figure 1, left). In Asia, maize production on the North China Plain is concentrated at similar temperatures. We therefore assume the Iowa growing period temperature is a de facto "optimum".

Expected warming in the corn belt by end of century is far larger than the current growing-season spread in temperatures. Using 4 representative models from ISIMIP (the InterSectoral Impact Model Intercomparison Project

Hempel et al., 2013) and the RCP8.5 forcing scenario, the average temperature rise over these same growing periods is over 5°C (Figure 1, bottom). This increase is over 60% greater than the global mean temperature change(3.6°C)Knutti and Sedláček (2013), as is expected for the continental mid-latitudes where the corn belt and other breadbaskets lie (e.g. Holland and Bitz, 2003). Even in a strong emission-reduction scenario (CMIP6-SSP126), mean corn belt warming in these models is as high as ∼5°C (CMIP6 O'Neill et al., 2016) by end of century (Supplemental Figure S4-S5). The high-end warming could translate into a poleward shift of maize cultivation by more than 1000 km, if the growing season "optimum" temperatures are to remain constant, i.e. a relocation of the current maize belt to central Canada (Figure 1, right).

3.2 | Stasis in the no-adaptation case

Without adaption, crop models generally show little poleward movement of optimal growing regions (gridcells in the top 10% of simulated yields, regionally) under warming. For North American maize, in the no-adaptation (A0) GGCMI Phase 2 6°C warming simulations, mean poleward movement of the breadbasket center averages only 1.3 degrees latitude or less than 150 kilometers across 6 of the 7 models. (The pDSSAT model is an outlier both in temperature sensitivity and in changes in spatial patterns, and shows a shift of nearly 900 km.) All crop models show overall yield losses under warming, so that the maize breadbasket becomes less productive, but in all but pDSSAT, the current region of highest yield largely remains the optimum land. As an illustration we show simulation results from a single model, GEPIC (Figure 2). (See Supplemental Figures S6-S19 for other models, which show qualitatively similar results.) Under current climate conditions, simulated potential maize yields vary widely across North America given the diversity of climate and soils (Figure 2a, blue), with the highest potential yields in the real-world area of most intensive cultivation (Figure 2a, pink). Under 6°C warming, the yield distribution contracts and maize yields above 6 ton ha^{-1} almost entirely disappear. That is, yield declines across the "breadbasket" area are not paired with yield increases elsewhere, so the current Midwestern "breadbasket" remains the top-yielding region, although its productivity is lower. The slight net poleward movement of the model maize breadbasket (1.2 degrees or 133 km) is largely driven by more severe losses in the high-yielding Gulf Coast than in the Midwestern corn belt (Figure 2, insets), likely due to non-linear temperature impacts. (Losses in the Gulf Coast also contribute to the anomalous poleward breadbasket shift in pDSSAT; see Discussion and Supplemental Figure S8.)

The result that breadbaskets remain fixed in the absence of adaptation is robust across assumptions about [CO_2] and water stress. Because CO_2 impacts are largely uniform across latitude, they can do little to modify the location of the "breadbasket" under warming. Using 810 ppm in the GGCMI Phase 2 +6°C warming simulations mitigates yield losses and can produce a slight westward shift of the breadbasket, presumably because elevated [CO_2] protects against water stress (Supplemental Figure S6), but poleward shifts are even smaller than in the constant [CO_2] case: only 1.1 degrees in the 6-model average. For pDSSAT, the poleward shift is essentially identical for both [CO_2] levels (See Supplemental Figures S6–S19). Similarly, breadbasket location remains fixed in simulations without water stress (the GGCMI Phase 2 fully irrigated case) (Supplemental Figure S7). Unlimited irrigation produces a more westward breadbasket in all climate conditions, and mitigates yield losses under warming.

Results are also robust across crops and locations. Figure 3 shows an estimate of latitudinal-average total production for maize, soybean, wheat, and rice in both present-day and +6°C conditions. (To restrict production to plausibly cultivated land, we use only gridcells exceeding the global median for each model, then take the multi-model mean.) Warmer temperatures reduce production at most latitudes, with mild gains in northern regions for all crops other than wheat, which is further impacted by switching between winter and spring wheat. Northern gains are however not large enough to substantially modify the latitude of peak productivity. In the N. hemisphere, the poleward shift in

peak productivity (total for a given latitude band) under +6°C warming is 2.5 degrees latitude (280 km) for maize, 0.4 (45 km) for wheat, 0.1 (10 km) for rice, and 3.6 (390 km) for soybean in the multi-model mean. (In the S. hemisphere, poleward motion of peak productivity regions is limited by lack of land). In simulations where warming is combined with high levels of [CO_2], the poleward shift in peak productivity under warming is even smaller: 2.3 degrees latitude for maize, 0.4 for wheat, -0.2 for rice and 3.2 for soybeans in the multi-model mean (Supplemental Figure S21, for the +6°C, 810 ppm [CO_2] case). Higher [CO_2] levels effectively eliminate warming-induced losses everywhere outside the tropics, but gains at high latitude remain too small to substantially shift zones of peak productivity.

3.3 | Growing season adaptation allows geographic shifts

Inclusion of adaptive measures in warmer climate conditions produces dramatic changes in projections of both yield amounts and their spatial distribution, in all models other than pDSSAT. While crop model breadbaskets barely move under warming in the no-adaptation (A0) case (Figure 4a, yellow arrows), the same models produce significant shifts in the adaptation (A1) case (Figure 4a, red arrows). In the GGCMI Phase 2 simulations, all models have a harmonized growing season of ~135 days under current conditions for the N. American maize breadbasket (ranging from ~130 days in Southern Illinois to ~140 days in North Dakota). In the A0 simulations, the growing season contracts in warmer conditions in all models, losing an average of 33 days at T+6 C, or 25% of its total length. Shortened growing seasons under warming result because plant maturation is tightly related to total accumulated heat, and contribute to steep yield losses averaging 31% over the breadbasket. Because yields decline everywhere, moving maize cultivation slightly north to the new optimal location can recover only a few percent of warming-related losses (Figure 4b-c, yellow bars). In the GGCMI Phase 2 A1 simulations, model parameters are adjusted to retain growing season length, representing adaptation by using new cultivars with delayed maturity. Cultivar adaptation alone recovers on average 68% of the temperature-driven loss seen in the A0 case, even if cultivation area is held fixed (Figure 4b-c, blue bars; see also (Zabel et al., 2021) in this issue). Because areas further north actually rise in yield, the optimal location for maize cultivation in North America shifts north by on average 3.1 degrees latitude (340 km) excluding pDSSAT, or 3.3 degrees (370 km) across all models. Allowing maize cultivation to move north to its new optimum location further reduces losses related to climate change, by an average of 91% across models. These results are qualitatively similar across degrees of warming (Supplemental Figure S23 shows the +2°C case), and whether or not [CO_2] is assumed to rise with warming. When warming of +6°C is combined with [CO_2] rising to 810 ppm (Supplemental Figure S24), the breadbasket shift in cultivar-adaptation A1 scenarios is 2.4 degrees (266 km), vs. 1.1 degrees (120 km) in the no-adaptation A0 runs (excluding pDSSAT).

Although breadbaskets do move substantially in the GGCMI adaptation (A1) simulations, they still shift less than would be expected in a "climate suitability" framework. In the +6°C applied warming scenario, the mean N. American maize breadbasket would have to shift by over 800 km to maintain a constant growing-season temperature (Figure 4a, white arrow). The realized shift of 340 km in the A1 case (for all models excluding pDSSAT) mitigates only 3.5°C of warming. (In the temperature-sensitive pDSSAT, its larger geographic shift mitigates all but 0.6°C of warming.) One potential explanation is that the A1 simulations only partially capture farmer adaptation. In A1, delayed-maturity cultivars allow retaining present growing-season length in each location, but in reality farmers would *extend* growing seasons to take advantage of earlier frost-free conditions. The A1 specifications artificially leave planting and harvest dates unchanged even in warmer conditions. We therefore turn to new simulations with the LPJmL model to explore the full set of factors that may affect changes in spatial yield distributions under warming.

The LPJmL model allows incorporating rule-based growing season adaptions in addition to a crop maturity delay. We consider an extended set of simulations including four adaptation cases. In *planting advance*, planting dates are

allowed to advance with warming but cultivar choice is unchanged. In *maturity delay*, cultivar adaptation maintains growing period length but planting date is unchanged, analogous to A1. In *plant & maturity*, both adaptations, and, for comparison, in *soils & radiation* full adaptation is combined with uniform soils and radiation set to values in Iowa, the presumed optimum. Simulations over present-day and warmer future conditions are run using output from 4 climate models as described in Methods; we show HadGEM2 results here, in which the mean future warming of the historical N. American maize breadbasket and growing season is 6.7°C. As expected, the LPJmL runs are consistent with the conclusion that in the absence of growing season adaptations, optimal growing locations do not shift (Figure 5). In the LPJmL *no-adaptation* case under HadGEM2, the N. American maize breadbasket moves only slightly poleward, by 55 km, and experiences nearly the full extent of unmitigated warming, 5.25°C out of 5.28°C in the original location (Figure 5, grey), and severe yield losses at -20%. Note that this temperature differs from the 6.7°C given above because the growing season contracts dramatically, by more than 5 weeks or ~30%, so that harvest occurs in late July instead of early September. See Supplemental Table S1 for growing season details and yield losses for all cases.

Growing season adaptations appear critical in allowing the optimal maize production location to shift under warming, with geographic factors playing a lesser role. Allowing *maturity delay* adaptation produces a strong poleward shift by nearly 610 km, larger than in the analogous GGCMI Phase 2 A1 simulations (Figure 5, green), but only weakly mitigates warming, since in these more realistic climate simulations the meridional temperature gradient flattens. Because high latitudes warm more strongly than mid-latitudes, displacing cultivation poleward is less effective at lowering growing season temperatures than in GGCMI Phase 2 where temperature offsets are uniform. Yield losses are then nearly as great as in the *no-adaptation* case, at -15%. In the *planting advance* case, the poleward shift is more moderate, at 400 km (Figure 5, olive). Growing season temperature rise is however kept to only 1.9°C by a combination of severe advancement of the growing season (by three weeks, so that planting occurs in early April instead of early May) and contraction of the growing season (by over a month, so that harvest now occurs in early July). Yield losses remain severe at -15%.

Substantial avoidance of yield losses occurs only when both growing season adaptation strategies are adopted simultaneously, so that warming can be reduced while maintaining growing season length. In the *plant & maturity* case (Figure 5, teal), peak yields move poleward by 780 km, planting dates remain advanced, and mean growing season becomes actually longer than in the baseline case, so that harvest occurs in late August. The longer time to maturity means the growing-season mean temperature is warmer than in *planting advance*, at 2.8°C, but yields are substantially higher, at net gains of 3% from the baseline case. Finally, removing constraints imposed by soils and radiation boosts the poleward breadbasket shift and yield gain only slightly, suggesting these are not the major constraints (Figure 5, blue). Using Iowa *soils & radiation* conditions everywhere moves the optimum production region an additional 130 km polewards, reduces net warming to 2.3°C, and increases yields to 6% above baseline.

Note that even the maximum breadbasket shift in Figure 5 is still only about half that required to produce a "temperature analogue" to present-day conditions, as in the climate suitability framework. It may in fact be geographically impossible for cultivation to shift sufficiently to avoid all warming, since in these realistic climate projections the temperature analogue moves twice as far as in the GGCMI Phase 2 simulations of Figure 4. Nevertheless, growing season adaptations in LPJmL are sufficient to retain yields. These results are qualitatively similar for all 4 climate models tested, even though amounts and patterns of warming differ (Figure S25). While Figure 5 shows the fixed-[CO_2] simulations, shifts are nearly identical in the dynamic-[CO_2] case, although yields improve (Figure S25, see also Figures S26–30 for spatial distributions of LPJmL yields in each climate simulation).

These results are broadly consistent across other major global breadbaskets. Figure 6 highlights the shift of the top breadbasket for each of four crops included in this analysis under both *no adaptation* (top) and the fully adapted *plant & maturity* (bottom) simulations. In all crops other than soybean, breadbaskets remain almost stationary under

warming in the absence of growing season adaptation, or even move slightly equatorwards. The exception is S. American soybean, whose optimal production location moves strongly poleward, but this case is also the exception in that the breadbasket lies in the subtropics (21 S) rather than mid-latitudes, where precipitation rather than temperature typically drives the spatial distribution of yields. With full growing season adaptation, all breadbaskets move moderately to strongly polewards. Both maize and soybean breadbaskets shift by nearly 800 km. Rice cultivation in Asia is constrained by land availability, since simulations were run only over areas where irrigation is feasible (excluding deserts), and moves only ~500 km. European wheat exhibits the weakest shift, ~350 km, again in part from land considerations: wheat cultivation is already centered so far north (50 N) that limited lands exists for further poleward displacement (Figure 6c,g). See Supplemental Table S2 for summary statistics for all crops.

4 | DISCUSSION

In experiments with multiple crop models, inclusion or omission of adaptive measures substantially impacts the location of optimal grain production. Breadbaskets do not move poleward under warming if changes in planting date and cultivar genetics are not permitted, but do shift substantially given these adaptations, with the largest response resulting from cultivar changes to delay maturity. With full growing season adaptation, the projected shift in the North American maize belt by end of century under the RCP8.5 scenario is almost 800 km (approximately 10x the shift observed since 1973 in Sloat et al. (2020)). Yields are recovered only in full adaptation simulations that allow both adopting new genetics and adjusting sowing dates: both adaptations appear required to fully capitalize on the temperature increase at higher latitudes. These results are common to nearly all crop models and are robust to the level of warming, whether simulations apply uniform warming or more realistic patterns, and whether [CO_2] fertilization is or is not considered. As expected shifts appear slightly greater in cases with uniform warming (as in the GGCMI experiment) than in those with more 'realistic' climate scenarios with amplified high-latitude warming. In no cases, however, do breadbaskets shift sufficiently to follow the temperature analog, even when constraints of soils and radiation are removed. Water availability could play some role in limiting poleward shifts, but note that *changes* in precipitation do not, since the four climate models tested do not show consistent latitudinal differences in precipitation changes. (See Supplemental Section S1 for details.)

Although the crop models used in this work produce qualitatively similar results, it is not yet possible to quantitatively predict future breadbasket locations. While the inclusion of adaptation in crop models is an advance on assuming static growing seasons, as is often done in global-scale crop model experiments (e.g. Rosenzweig et al., 2014), all versions shown here are still simplified. In LPJmL, the rules used to determine planting dates and cultivars use only one of either temperature or precipitation, depending on mean seasonal characteristics (Waha et al., 2012; Minoli et al., 2019a), and neglect considerations of intra-annual variability as well as soil moisture dynamics that can constrain planting dates. Furthermore, while planting dates are adjusted in each individual year, cultivar choice is based on 20-year mean climate and is not adjusted in years where planting is earlier or later. The model does not take account of management issues like the need for double-cropping, or potential limitations in the availability of ideal cultivars for future climate conditions (e.g. Zabel et al., 2021, this issue). In general, many crop models do not have a sophisticated enough soil representation to capture all limitations imposed by poor soil quality, as in the thin-soiled Laurentian Shield of the Upper Midwest and Canada. Finally, the 50-km horizontal resolution of this study may not be suitable in cases where agriculture moves to higher *altitudes* under warming, a potentially important adaptation pathway (e.g Läderach et al., 2017).

Crop models also show intrinsic differences in the growing season responses to warming that drive the need for

adaptations. The GGCMI Phase 2 crop simulations differ in the contraction of growing seasons in the no-adaptation case, and, especially at high latitudes, in the ability of cultivar changes to recover original growing seasons. In general, models show the strongest agreement in currently-cultivated areas, and the largest spread in the high-latitude areas where breadbaskets may move (Supplemental Figure S32). Treatment of model calibration may also be a source of differences in model projections of breadbasket shifts. While most GGCMI Phase 2 models are uniformly uncalibrated, the outlier in this analysis, pDSSAT, was calibrated in those regions where yield data exists. This difference may contribute to the stronger temperature sensitivity of pDSSAT maize (Franke et al., 2020b), and in turn in the greater poleward displacement of its breadbasket.

While this study focuses on changes in potential yields, it is also worth noting that the spatial distribution of agriculture today depends on many other factors. In many places, food is grown where people live, meaning that much current cultivation occurs in sub-optimum conditions (e.g. Nelson et al., 2010). Areas of intense cultivation also often relate to national borders, whether because of cultural factors or through strategic choices to maintain domestic production. (See e.g. local cultivation peaks in India and Indonesia in Figure 3.) Simulated shifts in breadbaskets across national borders may not materialize for the same reasons that have established patterns of cultivated areas today. (See Supplemental Table S3 for transnational shifts in LPJML.) Even within individual countries, production of many crops are physically constrained by geography: for example, rice in Indonesia, wheat in Southern Australia, or any crop in Northern India or South Africa. (See Supplemental Figure S31 for shifts in African breadbaskets.) Finally, cultivation of one crop can affect others. For example, soybean is often planted in areas that may be warmer than biologically optimal, because it is rotated with maize for restoring soil nutrients. All these considerations mean that adaptation by shifting cultivation may be limited – that is, in future warmer conditions, cultivation may not shift as much as do potential yields.

The results of this study nevertheless suggest important lessons for understanding the effect of climate change on food production. Agricultural climate impacts assessments to date have typically focused on currently-cultivated land and generally omit adaptive measures. This is necessarily true for studies based on statistical models (e.g. Schlenker and Roberts, 2009; Hsiang et al., 2017), and those using process-based models have largely followed similar practices (e.g. Rosenzweig et al., 2014; Moore et al., 2017a; Jägermeyr et al., 2021). More recently, some studies have included cultivar adaptations (e.g. Asseng et al., 2019), but do not include changes in planting dates. Current assessments are therefore likely overly pessimistic, both overestimating damages where crops are currently grown and not allowing shifting cultivation to higher-yielding areas. These issues in turn compromise economic studies that build on these assessments to estimate changes in regional agricultural competitiveness (e.g. Stevanović et al., 2016; Janssens et al., 2020). This work highlights the complexity of capturing agricultural responses to climate change, and the limitations of "shortcuts" in analysis: neither assumptions of stasis nor simple climate suitability frameworks appear to apply. Furthermore, understanding the displacement of breadbaskets is intrinsically important, because the climate threat to the food system lies not only in reductions in total food production, but in disruptions to where that production happens. If adaptive measures substantially change both yields and spatial yield patterns under climate change, accurately capturing agricultural responses requires global analyses using process-based models that explicitly represent these management choices. Such efforts are more difficult, and may require large interdisciplinary teams, but appear to be the only pathway to understanding climate risks to the global food system.

Acknowledgments

The authors thank the rest of AgMIP and GGCMI research teams and Frances Moore for helpful comments. Computing resources were provided by the University of Chicago Research Computing Center. This work was supported in part

by the U. Chicago Center for Robust Decision-making on Climate and Energy Policy (RDCEP), funded by NSF grant SES-1463644 through the Decision Making Under Uncertainty program. James Franke was supported by the NSF NRT program (grant DGE-1735359) and the NSF Graduate Research Fellowship Program (grant DGE-1746045). Sara Minoli was supported by the AXIS project MAPPY (01LS1903A) funded through the German Federal Ministry of Education and Research (BMBF). Haynes Stephens was was supported by the NSF NRT program (grant DGE-1735359). Alex Ruane was supported by NASA NNX16AK38G (INCA) and the NASA Earth Sciences Directorate/GISS Climate Impacts Group. Christian Folberth was supported by the European Research Council Synergy (grant no. ERC-530 2013-SynG-610028 Imbalance-P). Stefan Olin acknowledges support from the Swedish strong research areas BECC and MERGE, together with support from LUCCI (Lund University Centre for studies of Carbon Cycle and Climate Interactions).

Author contribution

E.M., J.F., and C.M. designed the research. C.M., J.E., and A.R. supervised the simulations. C.M., J.E., C.F., R.C.I.,C.J., J.J., T.H., W.L., S.M., S.O., T.A.M.P., and F.Z. performed the simulations. J.F., C.G., and H.S. performed the analysis. J.F., E.M., and C.M. prepared the manuscript. All authors contributed to the interpretation of results, writing, and review of the manuscript.

Conflict of interest

The authors declare no competing interests.

Data availability

All data used in this analysis are publicly available. Simulation outputs from GGCMI phase 2 are available on at `https://zenodo.org/search?page=1&size=20&q=GGCMI`. CMIP5 climate model outputs are publicly available at ISIMIP `https://data.isimip.org/`. AgMERRA data is available at reference: (Ruane et al., 2015). SPAM data is available at reference: (International Food Policy Research Institute, 2019). LPJmL RCP8.5 simulation outputs and code for analysis and figures are available upon request to the authors.

ORCIDs

James A. Franke: https://orcid.org/000-0001-8598-750X
Christoph Müller: https://orcid.org/0000-0002-9491-3550
Jonas Jägermeyr: https://orcid.org/0000-0002-8368-0018
Alex C. Ruane: https://orcid.org/0000-0002-5582-9217
Sara Minoli: https://orcid.org/0000-0001-7920-3107
Florian Zabel: https://orcid.org/0000-0002-2923-4412
Haynes Stephens: https://orcid.org/0000-0002-2258-5244
Thomas A.M. Pugh: https://orcid.org/0000-0002-6242-7371
Stefan Olin: https://orcid.org/0000-0002-8621-3300
R. Cesar Izaurralde: https://orcid.org/0000-0002-8797-9500
Wenfeng Liu: https://orcid.org/0000-0002-8699-3677

Curtis D. Jones: https://orcid.org/0000-0002-4008-5964

Supporting Information

Supporting information can be found at (link to be inserted by Journal) (pdf attached).

references

Akpoti, K., Kabo-bah, A. T. and Zwart, S. J. (2019) Agricultural land suitability analysis: State-of-the-art and outlooks for integration of climate change analysis. *Agricultural Systems*, **173**, 172–208. URL: https://linkinghub.elsevier.com/retrieve/pii/S0308521X18300428.

Anderson, W. B., Seager, R., Baethgen, W., Cane, M. and You, L. (2019) Synchronous crop failures and climate-forced production variability. *Science Advances*, **5**, eaaw1976. URL: https://advances.sciencemag.org/lookup/doi/10.1126/sciadv.aaw1976.

Asseng, S., Ewert, F., Martre, P., Rötter, R. P., Lobell, D. B., Cammarano, D., Kimball, B. A., Ottman, M. J., Wall, G. W., White, J. W., Reynolds, M. P., Alderman, P. D., Prasad, P. V. V., Aggarwal, P. K., Anothai, J., Basso, B., Biernath, C., Challinor, A. J., De Sanctis, G., Doltra, J., Fereres, E., Garcia-Vila, M., Gayler, S., Hoogenboom, G., Hunt, L. A., Izaurralde, R. C., Jabloun, M., Jones, C. D., Kersebaum, K. C., Koehler, A.-K., Müller, C., Naresh Kumar, S., Nendel, C., O'Leary, G., Olesen, J. E., Palosuo, T., Priesack, E., Eyshi Rezaei, E., Ruane, A. C., Semenov, M. A., Shcherbak, I., Stöckle, C., Stratonovitch, P., Streck, T., Supit, I., Tao, F., Thorburn, P. J., Waha, K., Wang, E., Wallach, D., Wolf, J., Zhao, Z. and Zhu, Y. (2015) Rising temperatures reduce global wheat production. *Nature Climate Change*, **5**, 143–147. URL: http://www.nature.com/articles/nclimate2470.

Asseng, S., Martre, P., Maiorano, A., Rötter, R. P., O'Leary, G. J., Fitzgerald, G. J., Girousse, C., Motzo, R., Giunta, F., Babar, M. A., Reynolds, M. P., Kheir, A. M. S., Thorburn, P. J., Waha, K., Ruane, A. C., Aggarwal, P. K., Ahmed, M., Balkovič, J., Basso, B., Biernath, C., Bindi, M., Cammarano, D., Challinor, A. J., De Sanctis, G., Dumont, B., Eyshi Rezaei, E., Fereres, E., Ferrise, R., Garcia-Vila, M., Gayler, S., Gao, Y., Horan, H., Hoogenboom, G., Izaurralde, R. C., Jabloun, M., Jones, C. D., Kassie, B. T., Kersebaum, K.-C., Klein, C., Koehler, A., Liu, B., Minoli, S., Montesino San Martin, M., Müller, C., Naresh Kumar, S., Nendel, C., Olesen, J. E., Palosuo, T., Porter, J. R., Priesack, E., Ripoche, D., Semenov, M. A., Stöckle, C., Stratonovitch, P., Streck, T., Supit, I., Tao, F., Van der Velde, M., Wallach, D., Wang, E., Webber, H., Wolf, J., Xiao, L., Zhang, Z., Zhao, Z., Zhu, Y. and Ewert, F. (2019) Climate change impact and adaptation for wheat protein. *Global Change Biology*, **25**, 155–173. URL: https://onlinelibrary.wiley.com/doi/abs/10.1111/gcb.14481.

Bagley, J. E., Desai, A. R., Dirmeyer, P. A. and Foley, J. A. (2012) Effects of land cover change on moisture availability and potential crop yield in the world's breadbaskets. *Environmental Research Letters*, **7**, 014009. URL: https://iopscience.iop.org/article/10.1088/1748-9326/7/1/014009.

Batjes, N. (2016) Harmonized soil property values for broad-scale modelling (wise30sec) with estimates of global soil carbon stocks. *Geoderma*, **269**, 61 – 68. URL: https://doi.org/10.1016/j.geoderma.2016.01.034.

Blasing, T. J. and Solomon, A. M. (1983) Response of the north american corn belt to climatic warming. In *Conference on interactions between climate and biosphere, Osnabruck, F.R. Germany, 21 Mar 1983*.

von Bloh, W., Schaphoff, S., Müller, C., Rolinski, S., Waha, K. and Zaehle, S. (2018) Implementing the nitrogen cycle into the dynamic global vegetation, hydrology, and crop growth model LPJmL (version 5.0). *Geoscientific Model Development*, **11**, 2789–2812. URL: https://www.geosci-model-dev.net/11/2789/2018/.

Caviezel, C., Hunziker, M. and Kuhn, N. (2017) Bequest of the Norseman—The Potential for Agricultural Intensification and Expansion in Southern Greenland under Climate Change. *Land*, **6**, 87. URL: http://www.mdpi.com/2073-445X/6/4/87.

Challinor, A. J., Müller, C., Asseng, S., Deva, C., Nicklin, K. J., Wallach, D., Vanuytrecht, E., Whitfield, S., Ramirez-Villegas, J. and Koehler, A.-K. (2018) Improving the use of crop models for risk assessment and climate change adaptation. *Agricultural Systems*, **159**, 296–306. URL: https://linkinghub.elsevier.com/retrieve/pii/S0308521X16307703.

Costinot, A., Donaldson, D. and Smith, C. (2016) Evolving Comparative Advantage and the Impact of Climate Change in Agricultural Markets: Evidence from 1.7 Million Fields around the World. *journal of political economy*, 44.

Elliott, J., Kelly, D., Chryssanthacopoulos, J., Glotter, M., Jhunjhnuwala, K., Best, N., Wilde, M. and Foster, I. (2014) The parallel system for integrating impact models and sectors (pSIMS). *Environmental Modelling & Software*, **62**, 509–516. URL: https://linkinghub.elsevier.com/retrieve/pii/S1364815214001121.

Elliott, J., Müller, C., Deryng, D., Chryssanthacopoulos, J., Boote, K. J., Büchner, M., Foster, I., Glotter, M., Heinke, J., Iizumi, T., Izaurralde, R. C., Mueller, N. D., Ray, D. K., Rosenzweig, C., Ruane, A. C. and Sheffield, J. (2015) The Global Gridded Crop Model Intercomparison: data and modeling protocols for Phase 1 (v1.0). *Geoscientific Model Development*, **8**, 261–277. URL: https://www.geosci-model-dev.net/8/261/2015/.

Fischer, G., Nachtergaele, F., Prieler, S., van Velthuizen, H., Verelst, L. and Wiberg, D. (2008) Global Agro-ecological Zones Assessment for Agriculture (GAEZ).

Folberth, C., Elliott, J., Müller, C., Balkovič, J., Chryssanthacopoulos, J., Izaurralde, R. C., Jones, C. D., Khabarov, N., Liu, W., Reddy, A., Schmid, E., Skalský, R., Yang, H., Arneth, A., Ciais, P., Deryng, D., Lawrence, P. J., Olin, S., Pugh, T. A. M., Ruane, A. C. and Wang, X. (2019) Parameterization-induced uncertainties and impacts of crop management harmonization in a global gridded crop model ensemble. *PLOS ONE*, **14**, 1–36. URL: https://doi.org/10.1371/journal.pone.0221862.

Folberth, C., Gaiser, T., Abbaspour, K. C., Schulin, R. and Yang, H. (2012) Regionalization of a large-scale crop growth model for sub-Saharan Africa: Model setup, evaluation, and estimation of maize yields. *Agriculture, Ecosystems & Environment*, **151**, 21–33. URL: https://linkinghub.elsevier.com/retrieve/pii/S0167880912000497.

Food and Agriculture Organization of the United Nations (FAO) (2020) FAOSTAT database. URL: http://www.fao.org/faostat/en/home.

Franke, J. A., Müller, C., Elliott, J., Ruane, A. C., Jägermeyr, J., Balkovic, J., Ciais, P., Dury, M., Falloon, P. D., Folberth, C., François, L., Hank, T., Hoffmann, M., Izaurralde, R. C., Jacquemin, I., Jones, C., Khabarov, N., Koch, M., Li, M., Liu, W., Olin, S., Phillips, M., Pugh, T. A. M., Reddy, A., Wang, X., Williams, K., Zabel, F. and Moyer, E. J. (2020a) The GGCMI Phase 2 experiment: global gridded crop model simulations under uniform changes in CO2, temperature, water, and nitrogen levels (protocol version 1.0). *Geoscientific Model Development*, **13**, 2315–2336. URL: https://gmd.copernicus.org/articles/13/2315/2020/.

Franke, J. A., Müller, C., Elliott, J., Ruane, A. C., Jägermeyr, J., Snyder, A., Dury, M., Falloon, P. D., Folberth, C., François, L., Hank, T., Izaurralde, R. C., Jacquemin, I., Jones, C., Li, M., Liu, W., Olin, S., Phillips, M., Pugh, T. A. M., Reddy, A., Williams, K., Wang, Z., Zabel, F. and Moyer, E. J. (2020b) The GGCMI Phase 2 emulators: global gridded crop model responses to changes in CO₂, temperature, water, and nitrogen (version 1.0). *Geoscientific Model Development*, **13**, 3995–4018. URL: https://gmd.copernicus.org/articles/13/3995/2020/.

Gaupp, F., Hall, J., Hochrainer-Stigler, S. and Dadson, S. (2020) Changing risks of simultaneous global breadbasket failure. *Nature Climate Change*, **10**, 54–57. URL: http://www.nature.com/articles/s41558-019-0600-z.

Hank, T., Bach, H. and Mauser, W. (2015) Using a Remote Sensing-Supported Hydro-Agroecological Model for Field-Scale Simulation of Heterogeneous Crop Growth and Yield: Application for Wheat in Central Europe. *Remote Sensing*, **7**, 3934–3965. URL: http://www.mdpi.com/2072-4292/7/4/3934.

Hannah, L., Roehrdanz, P. R., K. C., K. B., Fraser, E. D. G., Donatti, C. I., Saenz, L., Wright, T. M., Hijmans, R. J., Mulligan, M., Berg, A. and van Soesbergen, A. (2020) The environmental consequences of climate-driven agricultural frontiers. *PLOS ONE*, **15**, e0228305. URL: https://dx.plos.org/10.1371/journal.pone.0228305.

He, Q. and Zhou, G. (2012) The climatic suitability for maize cultivation in China. *Chinese Science Bulletin*, **57**, 395–403. URL: http://link.springer.com/10.1007/s11434-011-4807-2.

Hempel, S., Frieler, K., Warszawski, L., Schewe, J. and Piontek, F. (2013) A trend-preserving bias correction – the ISI-MIP approach. *Earth System Dynamics Discussions*, **4**, 49–92. URL: https://esd.copernicus.org/articles/4/219/2013/esd-4-219-2013.html.

Hertel, T. (2018) Climate change, agricultural trade and global food security.the state of agricultural commodity markets (soco) 2018: Background paper 9. *Tech. rep.*, FAO. URL: http://www.fao.org/3/CA1929EN/ca1929en.pdf.

Hoffman, A., Kemanian, A. and Forest, C. (2020) The response of maize, sorghum, and soybean yield to growing-phase climate revealed with machine learning. *Environmental Research Letters*, **15**, 094013. URL: https://iopscience.iop.org/article/10.1088/1748-9326/ab7b22.

Holland, M. M. and Bitz, C. M. (2003) Polar amplification of climate change in coupled models. *Climate Dynamics*, **21**, 221–232. URL: http://link.springer.com/10.1007/s00382-003-0332-6.

Hsiang, S., Kopp, R., Jina, A., Rising, J., Delgado, M., Mohan, S., Rasmussen, D. J., Muir-Wood, R., Wilson, P., Oppenheimer, M., Larsen, K. and Houser, T. (2017) Estimating economic damage from climate change in the United States. *Science*, **356**, 1362–1369. URL: https://science.sciencemag.org/content/356/6345/1362.

Iizumi, T., Kotoku, M., Kim, W., West, P. C., Gerber, J. S. and Brown, M. E. (2018) Uncertainties of potentials and recent changes in global yields of major crops resulting from census- and satellite-based yield datasets at multiple resolutions. *PLOS ONE*, **13**, 1–15. URL: https://doi.org/10.1371/journal.pone.0203809.

International Food Policy Research Institute (2019) Global Spatially-Disaggregated Crop Production Statistics Data for 2010 Version 2.0. URL: https://doi.org/10.7910/DVN/PRFF8V.

Izaurralde, R., Williams, J., McGill, W., Rosenberg, N. and Jakas, M. Q. (2006) Simulating soil C dynamics with EPIC: Model description and testing against long-term data. *Ecological Modelling*, **192**, 362–384. URL: https://linkinghub.elsevier.com/retrieve/pii/S0304380005003571.

Jägermeyr, J., Müller, C., Ruane, A. C., Elliott, J., Balkovic, J., Faye, B., Franke, J. A., Folberth, C., Iizumi, T., Khabarov, N., Lange, S., Liu, W., Minoli, S., Okada, M., Phillips, M., Mialyk, O., Moyer, E. J., Rabin, S., Schneider, J. M., Schyns, J. F., Skalsky, R., Stella, T., Stephens, H., Webber, H., Zabel, F. and Rosenzweig, C. (2021) Climate change signal in agriculture emerges earlier in new generation of projections. *Nature Food, in review*. URL: https://www.researchsquare.com/article/rs-101657/v1.

Janssens, C., Havlík, P., Krisztin, T., Baker, J., Frank, S., Hasegawa, T., Leclère, D., Ohrel, S., Ragnauth, S., Schmid, E., Valin, H., Van Lipzig, N. and Maertens, M. (2020) Global hunger and climate change adaptation through international trade. *Nature Climate Change*, **10**, 829–835. URL: http://www.nature.com/articles/s41558-020-0847-4.

Jones, J., Hoogenboom, G., Porter, C., Boote, K., Batchelor, W., Hunt, L., Wilkens, P., Singh, U., Gijsman, A. and Ritchie, J. (2003) The DSSAT cropping system model. *European Journal of Agronomy*, **18**, 235–265. URL: https://linkinghub.elsevier.com/retrieve/pii/S1161030102001077.

King, M., Altdorff, D., Li, P., Galagedara, L., Holden, J. and Unc, A. (2018) Northward shift of the agricultural climate zone under 21st-century global climate change. *Scientific Reports*, **8**, 7904. URL: http://www.nature.com/articles/s41598-018-26321-8.

Knutti, R. and Sedláček, J. (2013) Robustness and uncertainties in the new CMIP5 climate model projections. *Nature Climate Change*, **3**, 369–373. URL: https://www.nature.com/articles/nclimate1716.

Kogo, B. K., Kumar, L., Koech, R. and Kariyawasam, C. S. (2019) Modelling Climate Suitability for Rainfed Maize Cultivation in Kenya Using a Maximum Entropy (MaxENT) Approach. *Agronomy*, **9**, 727. URL: https://www.mdpi.com/2073-4395/9/11/727.

Kornhuber, K., Coumou, D., Vogel, E., Lesk, C., Donges, J. F., Lehmann, J. and Horton, R. M. (2020) Amplified Rossby waves enhance risk of concurrent heatwaves in major breadbasket regions. *Nature Climate Change*, **10**, 48–53. URL: http://www.nature.com/articles/s41558-019-0637-z.

Läderach, P., Ramirez–Villegas, J., Navarro-Racines, C., Zelaya, C., Martinez–Valle, A. and Jarvis, A. (2017) Climate change adaptation of coffee production in space and time. *Climatic Change*, **141**, 47–62. URL: https://link.springer.com/article/10.1007/s10584-016-1788-9.

Lindeskog, M., Arneth, A., Bondeau, A., Waha, K., Seaquist, J., Olin, S. and Smith, B. (2013) Implications of accounting for land use in simulations of ecosystem carbon cycling in Africa. *Earth System Dynamics*, **4**, 385–407. URL: https://www.earth-syst-dynam.net/4/385/2013/.

Liu, J., Williams, J. R., Zehnder, A. J. and Yang, H. (2007) GEPIC – modelling wheat yield and crop water productivity with high resolution on a global scale. *Agricultural Systems*, **94**, 478–493. URL: https://linkinghub.elsevier.com/retrieve/pii/S0308521X0600196X.

Liu, W., Yang, H., Folberth, C., Wang, X., Luo, Q. and Schulin, R. (2016a) Global investigation of impacts of PET methods on simulating crop-water relations for maize. *Agricultural and Forest Meteorology*, **221**, 164–175. URL: https://linkinghub.elsevier.com/retrieve/pii/S0168192316301800.

Liu, W., Yang, H., Liu, J., Azevedo, L. B., Wang, X., Xu, Z., Abbaspour, K. C. and Schulin, R. (2016b) Global assessment of nitrogen losses and trade-offs with yields from major crop cultivations. *Science of The Total Environment*, **572**, 526–537. URL: https://linkinghub.elsevier.com/retrieve/pii/S0048969716317867.

Mauser, W., Klepper, G., Zabel, F., Delzeit, R., Hank, T., Putzenlechner, B. and Calzadilla, A. (2015) Global biomass production potentials exceed expected future demand without the need for cropland expansion. *Nature Communications*, **6**. URL: http://www.nature.com/articles/ncomms9946.

Minoli, S., Egli, D. B., Rolinski, S. and Müller, C. (2019a) Modelling cropping periods of grain crops at the global scale. *Global and Planetary Change*, **174**, 35–46. URL: https://linkinghub.elsevier.com/retrieve/pii/S092181811830362X.

Minoli, S., Müller, C., Elliott, J., Ruane, A. C., Jägermeyr, J., Zabel, F., Dury, M., Folberth, C., François, L., Hank, T., Jacquemin, I., Liu, W., Olin, S. and Pugh, T. A. M. (2019b) Global Response Patterns of Major Rainfed Crops to Adaptation by Maintaining Current Growing Periods and Irrigation. *Earth's Future*, **7**, 1464–1480. URL: https://onlinelibrary.wiley.com/doi/abs/10.1029/2018EF001130.

Moore, F. C., Baldos, U., Hertel, T. and Diaz, D. (2017a) New science of climate change impacts on agriculture implies higher social cost of carbon. *Nature Communications*, **8**. URL: http://www.nature.com/articles/s41467-017-01792-x.

Moore, F. C., Baldos, U. L. C. and Hertel, T. (2017b) Economic impacts of climate change on agriculture: a comparison of process-based and statistical yield models. *Environmental Research Letters*, **12**, 065008. URL: https://iopscience.iop.org/article/10.1088/1748-9326/aa6eb2.

Müller, C., Franke, J., Jägermeyr, J., Ruane, A. C., Elliott, J., Moyer, E., Heinke, J., Falloon, P. D., Folberth, C., Francois, L., Hank, T., Izaurralde, R. C., Jacquemin, I., Liu, W., Olin, S., Pugh, T. A. M., Williams, K. and Zabel, F. (2021) Exploring uncertainties in global crop yield projections in a large ensemble of crop models and CMIP5 and CMIP6 climate scenarios. *Environmental Research Letters*, **16**, 034040. URL: https://doi.org/10.1088/1748-9326/abd8fc.

Müller, C., Elliott, J., Chryssanthacopoulos, J., Arneth, A., Balkovic, J., Ciais, P., Deryng, D., Folberth, C., Glotter, M., Hoek, S., Iizumi, T., Izaurralde, R. C., Jones, C., Khabarov, N., Lawrence, P., Liu, W., Olin, S., Pugh, T. A. M., Ray, D. K., Reddy, A., Rosenzweig, C., Ruane, A. C., Sakurai, G., Schmid, E., Skalsky, R., Song, C. X., Wang, X., de Wit, A. and Yang, H. (2017) Global gridded crop model evaluation: benchmarking, skills, deficiencies and implications. *Geosci. Model Dev.*, 20.

Müller, C. and Robertson, R. D. (2014) Projecting future crop productivity for global economic modeling. *Agricultural Economics*, **45**, 37–50. URL: http://doi.wiley.com/10.1111/agec.12088.

Nelson, G. C., Rosegrant, M. W., Palazzo, A., Gray, I., Ingersoll, C., Robertson, R., Tokgoz, S., Zhu, T., Sulser, T. B., Ringler, C. et al. (2010) *Food security, farming, and climate change to 2050: scenarios, results, policy options*, vol. 172. Intl Food Policy Res Inst. URL: http://dx.doi.org/10.2499/9780896291867.

Newman, J. (1980) Climate Change Impacts on the Growing Season of the North American Corn Belt. *Biometeorology*, **7**, 128–142.

Olin, S., Schurgers, G., Lindeskog, M., Wårlind, D., Smith, B., Bodin, P., Holmér, J. and Arneth, A. (2015) Modelling the response of yields and tissue C : N to changes in atmospheric CO2; and N management in the main wheat regions of western Europe. *Biogeosciences*, **12**, 2489–2515. URL: https://www.biogeosciences.net/12/2489/2015/.

O'Neill, B. C., Tebaldi, C., van Vuuren, D. P., Eyring, V., Friedlingstein, P., Hurtt, G., Knutti, R., Kriegler, E., Lamarque, J.-F., Lowe, J., Meehl, G. A., Moss, R., Riahi, K. and Sanderson, B. M. (2016) The Scenario Model Intercomparison Project (ScenarioMIP) for CMIP6. *Geoscientific Model Development*, **9**, 3461–3482. URL: https://gmd.copernicus.org/articles/9/3461/2016/.

Parmesan, C. (2006) Ecological and Evolutionary Responses to Recent Climate Change. *Annual Review of Ecology, Evolution, and Systematics*, **37**, 637–669. URL: http://www.annualreviews.org/doi/10.1146/annurev.ecolsys.37.091305.110100.

Qin, Y., Abatzoglou, J. T., Siebert, S., Huning, L. S., AghaKouchak, A., Mankin, J. S., Hong, C., Tong, D., Davis, S. J. and Mueller, N. D. (2020) Agricultural risks from changing snowmelt. *Nature Climate Change*, **10**, 459–465. URL: http://www.nature.com/articles/s41558-020-0746-8.

Ramirez-Cabral, N. Y. Z., Kumar, L. and Shabani, F. (2017) Global alterations in areas of suitability for maize production from climate change and using a mechanistic species distribution model (CLIMEX). *Scientific Reports*, **7**, 5910. URL: http://www.nature.com/articles/s41598-017-05804-0.

Rosenzweig, C. (1985) Potential CO2-induced climate effects on North American wheat-producing regions. *Climatic Change*, **7**, 367–389. URL: http://link.springer.com/10.1007/BF00139053.

Rosenzweig, C., Elliott, J., Deryng, D., Ruane, A. C., Müller, C., Arneth, A., Boote, K. J., Folberth, C., Glotter, M., Khabarov, N., Neumann, K., Piontek, F., Pugh, T. A. M., Schmid, E., Stehfest, E., Yang, H. and Jones, J. W. (2014) Assessing agricultural risks of climate change in the 21st century in a global gridded crop model intercomparison. *Proceedings of the National Academy of Sciences*, **111**, 3268–3273. URL: http://www.pnas.org/lookup/doi/10.1073/pnas.1222463110.

Rosenzweig, C., Jones, J., Hatfield, J., Ruane, A., Boote, K., Thorburn, P., Antle, J., Nelson, G., Porter, C., Janssen, S., Asseng, S., Basso, B., Ewert, F., Wallach, D., Baigorria, G. and Winter, J. (2013) The Agricultural Model Intercomparison and Improvement Project (AgMIP): Protocols and pilot studies. *Agricultural and Forest Meteorology*, **170**, 166–182. URL: https://linkinghub.elsevier.com/retrieve/pii/S0168192312002857.

Ruane, A. C., Goldberg, R. and Chryssanthacopoulos, J. (2015) Climate forcing datasets for agricultural modeling: Merged products for gap-filling and historical climate series estimation. *Agricultural and Forest Meteorology*, **200**, 233–248. URL: https://linkinghub.elsevier.com/retrieve/pii/S0168192314002275.

Ruane, A. C., Rosenzweig, C., Asseng, S., Boote, K. J., Elliott, J., Ewert, F., Jones, J. W., Martre, P., McDermid, S. P., Müller, C., Snyder, A. and Thorburn, P. J. (2017) An AgMIP framework for improved agricultural representation in integrated assessment models. *Environmental Research Letters*, **12**, 125003. URL: http://stacks.iop.org/1748-9326/12/i=12/a=125003?key=crossref.46721bd10090407d43a764e8d12cd4d2.

Sacks, W. J., Deryng, D., Foley, J. A. and Ramankutty, N. (2010) Crop planting dates: an analysis of global patterns: Global crop planting dates. *Global Ecology and Biogeography*, no–no. URL: http://doi.wiley.com/10.1111/j.1466-8238.2010.00551.x.

Schlenker, W. and Roberts, M. J. (2009) Nonlinear temperature effects indicate severe damages to U.S. crop yields under climate change. *Proceedings of the National Academy of Sciences*, **106**, 15594–15598. URL: http://www.pnas.org/lookup/doi/10.1073/pnas.0906865106.

Shangguan, W., Dai, Y., Duan, Q., Liu, B. and Yuan, H. (2014) A global soil data set for earth system modeling. *Journal of Advances in Modeling Earth Systems*, **6**, 249–263. URL: http://doi.wiley.com/10.1002/2013MS000293.

Sloat, L. L., Davis, S. J., Gerber, J. S., Moore, F. C., Ray, D. K., West, P. C. and Mueller, N. D. (2020) Climate adaptation by crop migration. *Nature Communications*, **11**, 1243. URL: http://www.nature.com/articles/s41467-020-15076-4.

Stevanović, M., Popp, A., Lotze-Campen, H., Dietrich, J. P., Müller, C., Bonsch, M., Schmitz, C., Bodirsky, B. L., Humpenöder, F. and Weindl, I. (2016) The impact of high-end climate change on agricultural welfare. *Science Advances*, **2**, e1501452. URL: https://advances.sciencemag.org/lookup/doi/10.1126/sciadv.1501452.

Toreti, A., Deryng, D., Tubiello, F. N., Müller, C., Kimball, B. A., Moser, G., Boote, K., Asseng, S., Pugh, T. A. M., Vanuytrecht, E., Pleijel, H., Webber, H., Durand, J.-L., Dentener, F., Ceglar, A., Wang, X., Badeck, F., Lecerf, R., Wall, G. W., van den Berg, M., Hoegy, P., Lopez-Lozano, R., Zampieri, M., Galmarini, S., O'Leary, G. J., Manderscheid, R., Mencos Contreras, E. and Rosenzweig, C. (2020) Narrowing uncertainties in the effects of elevated CO2 on crops. *Nature Food*, **1**, 775–782. URL: http://www.nature.com/articles/s43016-020-00195-4.

USDA National Agricultural Statistics Service (2020) NASS quick stats. URL: https://quickstats.nass.usda.gov/.

Waha, K., van Bussel, L. G. J., Müller, C. and Bondeau, A. (2012) Climate-driven simulation of global crop sowing dates: Simulation of global sowing dates. *Global Ecology and Biogeography*, **21**, 247–259. URL: http://doi.wiley.com/10.1111/j.1466-8238.2011.00678.x.

Wang, S., Stefania Di tommaso, Jillian M. Deines and David B. Lobel (2020) Mapping twenty years of corn and soybean across the US Midwest using the Landsat archive. *Scientific Data*, **7**, 14.

Warrick, R. A. (1988) Carbon Dioxide, Climatic Change and Agriculture. *The Geographical Journal*, **154**, 221. URL: https://www.jstor.org/stable/633848?origin=crossref.

Weedon, G. P., Balsamo, G., Bellouin, N., Gomes, S., Best, M. J. and Viterbo, P. (2014) The WFDEI meteorological forcing data set: WATCH Forcing Data methodology applied to ERA-Interim reanalysis data. *Water Resources Research*, **50**, 7505–7514. URL: http://doi.wiley.com/10.1002/2014WR015638.

Zabel, F., Delzeit, R., Schneider, J. M., Seppelt, R., Mauser, W. and Václavík, T. (2019) Global impacts of future cropland expansion and intensification on agricultural markets and biodiversity. *Nature Communications*, **10**, 2844. URL: http://www.nature.com/articles/s41467-019-10775-z.

Zabel, F., Müller, C., Elliott, J., Minoli, S., Jägermeyr, J., Schneider, J. M., Franke, J. A., Moyer, E., Folberth, C., Francois, M. D. L., Liu, W., Pugh, T. A. M., Olin, S., Rabin1, S. S., Mauser, W., Hank, T. and Ruane, A. C. (2021) Large potential for crop production adaptation depends on available future varieties. *Global Change Biology*. URL: https://onlinelibrary.wiley.com/doi/10.1111/gcb.15649.

Zabel, F., Putzenlechner, B. and Mauser, W. (2014) Global Agricultural Land Resources – A High Resolution Suitability Evaluation and Its Perspectives until 2100 under Climate Change Conditions. *PLoS ONE*, **9**, e107522. URL: https://dx.plos.org/10.1371/journal.pone.0107522.

Zhang, Y., Wang, Y. and Niu, H. (2017) Spatio-temporal variations in the areas suitable for the cultivation of rice and maize in China under future climate scenarios. *Science of The Total Environment*, **601-602**, 518–531. URL: https://linkinghub.elsevier.com/retrieve/pii/S0048969717313402.

Zhao, C., Liu, B., Piao, S., Wang, X., Lobell, D. B., Huang, Y., Huang, M., Yao, Y., Bassu, S., Ciais, P., Durand, J.-L., Elliott, J., Ewert, F., Janssens, I. A., Li, T., Lin, E., Liu, Q., Martre, P., Müller, C., Peng, S., Peñuelas, J., Ruane, A. C., Wallach, D., Wang, T., Wu, D., Liu, Z., Zhu, Y., Zhu, Z. and Asseng, S. (2017) Temperature increase reduces global yields of major crops in four independent estimates. *Proceedings of the National Academy of Sciences*, **114**, 9326–9331. URL: http://www.pnas.org/lookup/doi/10.1073/pnas.1701762114.

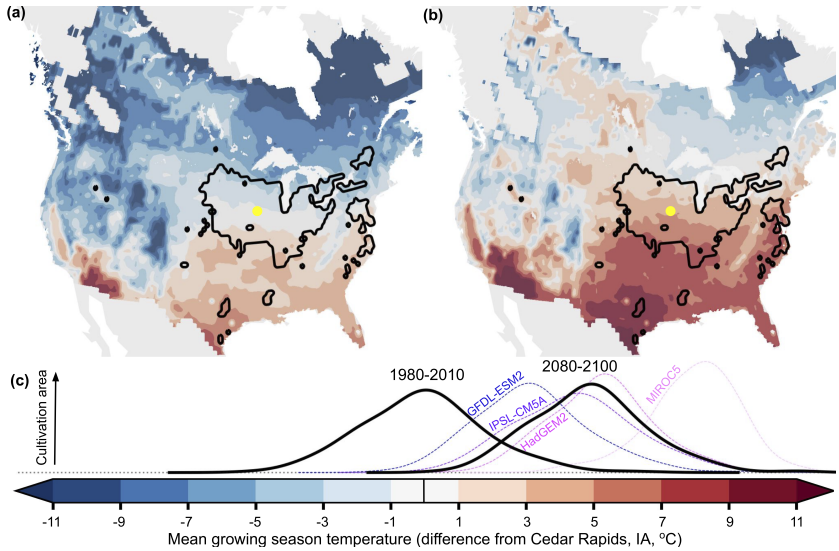

FIGURE 1 Poleward shift of optimum growing season temperatures under anthropogenic warming. Heat map shows the mean growing season temperature difference from the modal cultivated land for maize (Cedar Rapids, IA, for example - yellow dot) in **(a)** 1980-2010 **(b)** and the end of the century (2080-2100) under RCP8.5 for the InterSectoral Impact Model Intercomparison Project (ISIMIP-Fast track)-CMIP5 (Hempel et al., 2013) climate model mean. Growing seasons are taken from the GGCMI phase 2 crop calendar for each gridcell and held constant under warming. Black contours in (a, b) show gridcells with at least 10 kha cultivated in North America. **(c)** Temperature difference distribution of all breadbasket maize cultivated areas in North America historical mean conditions (1980-2010) and the end of the century (2080-2100, RCP8.5). Optimum growing season temperatures in the center of the bread basket may move between 500km (GFDL-ESM2, low sensitivity) to 1200km (MIROC5, high sensitivity) northward by the end of the century under warming.

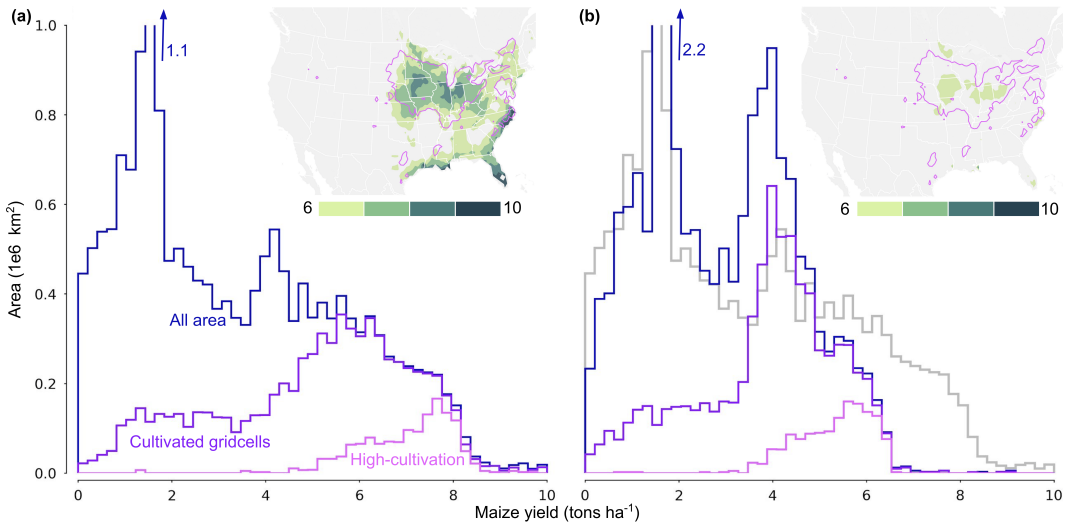

FIGURE 2 Breadbasket yields decline under warming while the latitude of peak yield remains fixed. Figure shows simulated yield across all land in North America in the GEPIC model for maize. Histogram lines indicate the median yield for all areas (blue), all areas with some cultivation (purple) and high-intensity cultivation areas (pink) for **(a)** 1980 - 2010 historical period and the **(b)** under 6°C of warming from the historical with constant [CO_2]. High-cultivation gridcells are those above 10 kha in North America. Inset plots show yields (in tons ha^{-1}) and the high-cultivation areas under the same conditions in each panel. Gray line in panel **(b)** shows the 1980-2010 distribution for all simulated areas. The highest simulated yields decline under warming and are not replaced at higher latitudes, therefore Iowa remains the best simulated maize yield in North America. See Supplemental Figures S6-19 for case with high [CO_2] and other models.

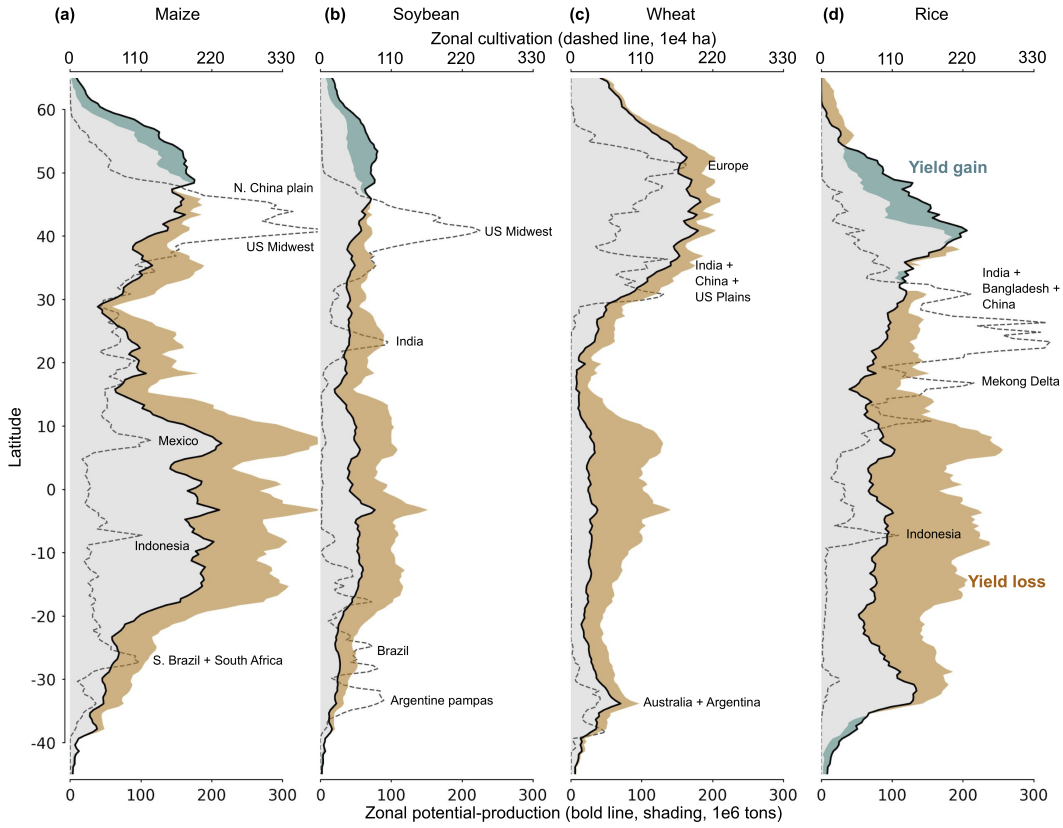

FIGURE 3 Warming-related changes in zonal potential grain production in the absence of adaptation, for maize **(a)**, soybean **(b)**, wheat **(c)**, and rice **(d)**, from GGCMI Phase 2 A0 crop model simulations. Values are total production in each 0.5 degree latitude band from all gridcells above global median yield, to approximate lands on which crops would reasonably be grown; values are calculated for each model and figure shows the multi-model mean. (See Supplemental Figure S21 for individual models.) Black line shows production under +6°C warming and brown and green areas the change from baseline climate conditions. Simulations are rainfed everywhere for all crops other than rice, which is irrigated everywhere. For reference, dashed line shows current actual total zonal cultivated area for each crop and labels mark regions of intense cultivation. Warming causes substantial losses at lower latitudes in all crops and some gains at high northern latitudes for all but wheat, but gains are not large enough to substantially shift the zones of optimal production at continental scale (e.g. N. American and Central American corn belts). Net production loss in wheat at high latitudes occurs because warming makes land unsuitable for high-producing winter wheat. (Wheat values here combine separate spring and winter simulations and take the better yield in each gridcell.) See Supplemental Figure S22 for simulations with elevated [CO_2], which show higher yields under warming but similar relative stasis of breadbaskets. Note that for crops other than rice, model peak production zones correspond to actual zones of intense cultivation, validating results. Real-world rice cultivation is constrained by availability of water and competition with higher-value maize and wheat.

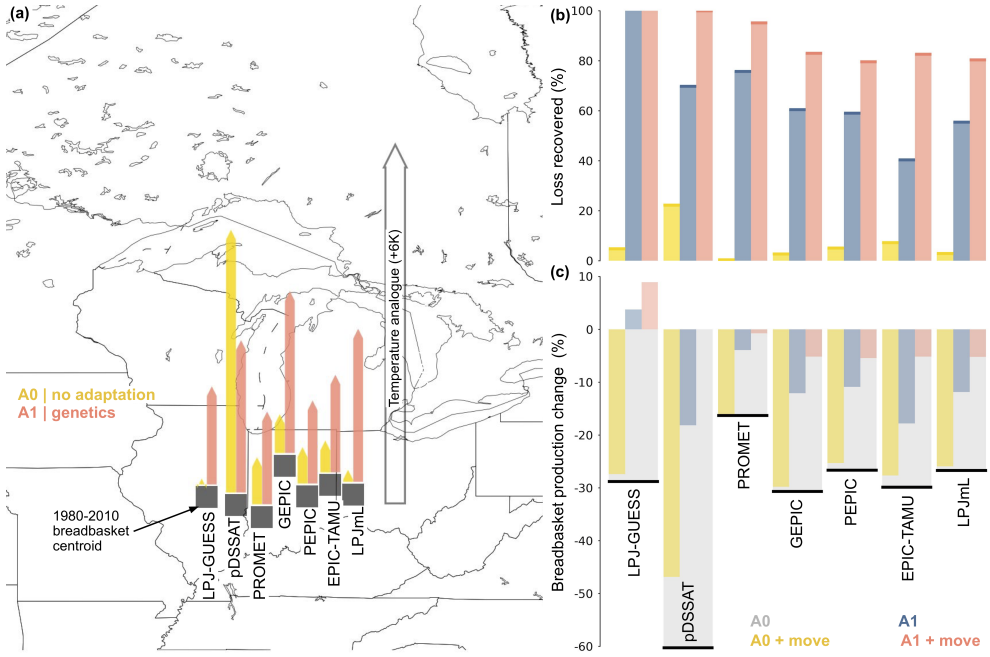

FIGURE 4 Effect of including cultivar adaptation on breadbasket location and productivity changes under warming, for N. American maize in the GGCMI Phase2 A0 (*no adaptation*) and A1 (*maturity delay*) simulations. Comparison shows baseline (1980-2010) climate and +6°C warming, [CO_2] of 360 ppm. Breadbasket are defined as described in text. **(a)** Mean latitude of the maize breadbasket for the 7 crop models and its poleward movement under warming for A0 (red) and A1 (yellow) simulations. Note that each model puts the historical breadbasket at a slightly different latitude, and longitudinal position has no meaning in this Figure.) All models other than pDSSAT, the high outlier in temperature response, show only slight poleward movement in A0 but substantial movement in A1. For comparison, white arrow marks the "climate analogue", the displacement in latitude required for the existing high-cultivation maize area to maintain its current growing season temperature. Even under A1, breadbaskets do not shift sufficiently to avoid warming. **(b)** Percent of temperature-driven production losses avoided by shifting cultivation locations alone (A0, yellow), by cultivar adaptation alone (A1, blue), and by both cultivars and movement (A1, red). Scale is truncated at 100%. Without cultivar adaptation, moving growing locations poleward has little benefit. Cultivar adaptation alone avoids 2/3 of warming-induced losses, and allowing relocation of cultivation further reduces losses. **(c)** Simulated maize production changes in the base +6°C warming case (grey = A0 + fixed cultivation) and under different adaptive measures (as in **b**). Changing both cultivars and locations reduces mean production losses from ~30% to <5%. See Supplemental Figures S23–24 for cases with +2°C warming and high [CO_2].

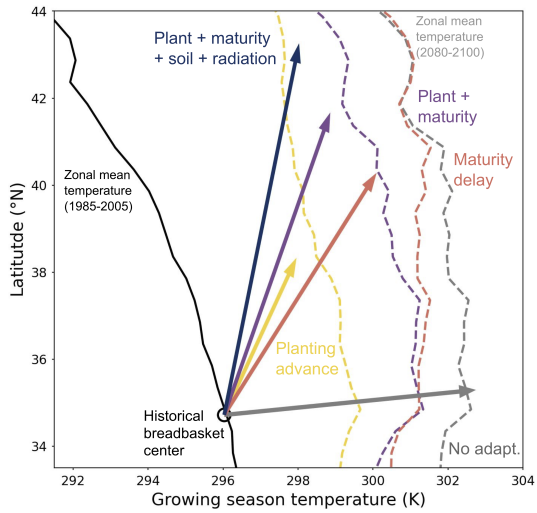

FIGURE 5 Changes in mean growing-season temperature and breadbasket location for N. American maize in LPJmL simulations with different adaptation strategies, as described in text. Arrows indicate breadbasket movement in temperature-latitude space by the end of the century in the HadGEM-2 RCP8.5 climate simulations. A vertical arrow would mean the optimal production location tracks with the temperature analogue. Dashed lines show zonal mean temperature rise at each 0.5 degree latitude band, for all N. American gridcells East of 100W. Note that climate projections flatten the meridional temperature gradient. Simulations show here use fixed [CO_2] for consistency; results are nearly identical in the dynamic [CO_2] case (Figure S25). With no adaptation (grey), breadbasket location remains nearly constant. All growing-season adaptations allow more substantial movement. Allowing earlier planting (olive) produces a moderate shift in breadbasket location and a much lower temperature rise, since early planting and accelerated maturity mean harvest occurs in mid-July instead of early September. Allowing delayed maturity (green, teal, blue) produces much larger breadbasket shifts but also warmer growing-season temperatures. Removing soil and radiation constraints (dark blue) contributes to poleward motion, even in this case total breadbasket shift is about half that required to produce a temperature analogue to present-day conditions.

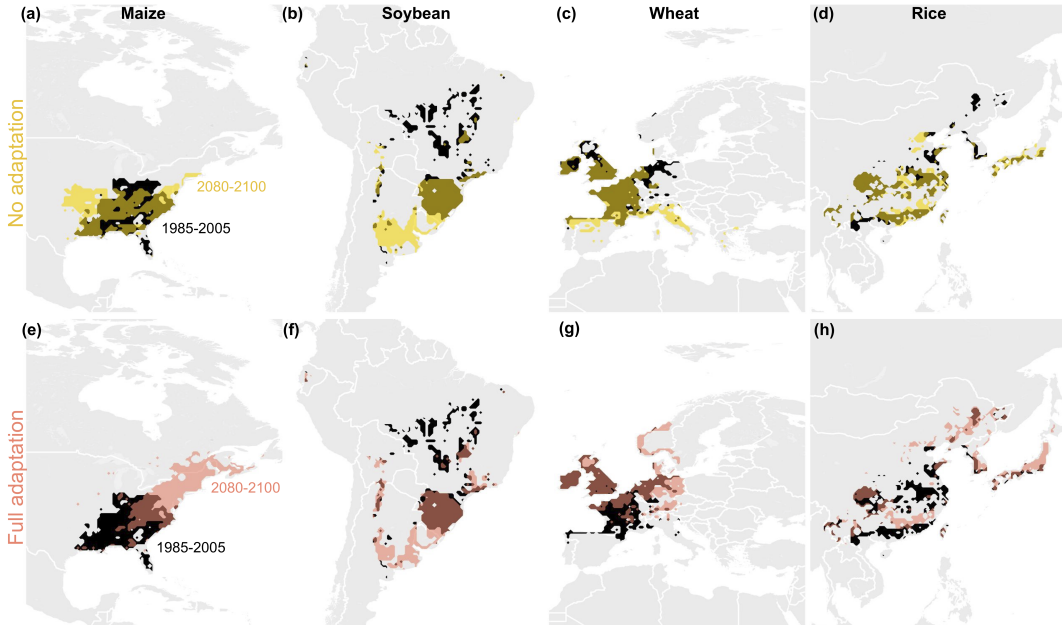

FIGURE 6 Regional differences in breadbasket shift. **(a-d)** historical top 10% regional yields (black) and end of the century top 10% of yields (gold) with fixed planting days and cultivar genetics for four crops and regions. **(e-h)** Same as top row now with fully-adapted growing seasons (planting advance and maturity delay). Simulations from LPJmL driven by the HadGEM-2 climate model under RCP8.5. South American soybeans move poleward to a further extent with fixed growing seasons than other crops. Wheat in Europe and Rice in East Asia both move poleward to a greater extent with dynamic seasons, but neither to the extent of North American Maize. See Section 2.2 for discussion about historical yield patterns.